

## Pore-Scale Study on Two-Phase Flow in Porous Media

Zhenyu LIU, Huiying WU\*

\* Corresponding author: Tel.: ++86 (021) 34205299; Fax: ++86 (021) 34205299; Email: whysrj@sjtu.edu.cn  
School of Mechanical Engineering, Shanghai Jiao Tong University, China

**Abstract** This paper presents currently available pore-scale predictive techniques for two-phase flow in porous media, which are based on the real description of the pore space. Two pore-scale models are established with FVM-VOF and LBM-VOF method based on the different complex foam structure, respectively. The two-phase flow of pore fluid is numerically simulated and the influence of the porous structure wettability is discussed based on the numerical predictions. These pore-scale models can be adopted to describe the detailed flow characteristic in porous media and evaluate their average effects.

**Keywords:** Pore Scale, Two-Phase Flow, FVM, LBM, VOF

### 1. Introduction

Two-phase flow in porous media widely exists in the industrial processes, such as enhanced oil recovery, carbon dioxide storage and proton exchange membrane fuel cells (PEMFC), etc. Macroscopic approaches are commonly adopted to describe the transport phenomena in porous media, which are based on the averaging pore-scale processes over the representative elementary volume (REV). The understanding of two-phase flow at the pore scale is of significant importance because the pore-scale characteristics of flow and heat transfer have a major influence on the macroscopic transport process. So the flow behavior on the pore scale is crucial for the prediction and design of above-mentioned industrial processes, which has been preliminarily studied by several researchers (Blunt et al., 2013; Jiao and Li, 2011; Xuan et al., 2011). The pore-scale study provides a bridge between the pore-scale and macro-scale representation, and it has attracted more and more attention in recent years (Sheng and Thompson, 2013).

The present available models to predict the immiscible flow in porous media have several options, such as Smoothed Particle Hydrodynamics (SPH), Finite Volume Method (FVM) or Lattice Boltzmann Method (LBM),

etc. Bandara et al. (2013) carried out a series of numerical experiments with the Pair-Wise Force Smoothed Particle Hydrodynamics (PF-SPH) multiphase flow model. They observed that unstable displacement occurs in both homogeneous and heterogeneous porous media at pore scale due to the hydrodynamic instability. Raeini et al. (2014) used a Volume-of-Fluid (VOF) based FVM to model two-phase flow through simple pore geometries and investigated the mechanisms controlling two-phase flow at the pore scale. But the geometries with non-uniform cross-sectional areas, the effects of fluid properties such as contact angle and viscosity ratios were not considered in their study. Jettestuen et al. (2013) presented a level set method to simulate the capillary controlled displacements with nonzero contact angles in porous media. They simulated quasi-static drainage and imbibition processes for different contact angles in several pore geometries, and capillary pressure and fluid/fluid specific interfacial area curves in each case were computed. A lattice Boltzmann high-density-ratio model, which uses diffuse interface theory to describe the interfacial dynamics, was extended to simulate immiscible multiphase flows in porous media by Liu et al. (2013). The model simulated the gas displacement of liquid in a homogenous two-dimensional pore network consisting of

uniformly spaced square obstructions. Pore-scale simulation of two-phase flows in a packed-sphere bed and in a carbon paper gas diffusion layer (GDL) was carried out using the free energy multiphase LBM by Hao and Cheng (2010).

Gunde et al. (2010) numerically simulated immiscible two-phase flow using Micro-CT scan image of a Berea Sandstone core, which displayed a two dimensional representation of pore network inside the scanned sample. Shokri et al. (2010) employed detailed imaging using x-ray synchrotron radiation to study liquid phase distribution and dynamics in the the domain below the surface of evaporating sand columns. Shahraeeni and Or (2012) used rapid x-ray synchrotron tomography measurements to resolve liquid-vapor interfacial dynamics during phase change process within sub-millimetric pores forming among sintered glass bead samples. The experimental techniques for two-phase flow in porous media are influenced by the resolution ratio of the scanning equipment and the limit of scanning time. Its cost is high and still not available in the real industrial field.

The FVM-VOF method is more popular because it has been developed for more than 30 years. Its application in porous media at pore scale has attracted more attention based on the recent reports. The LBM is very suitable to simulate the flow in the complex geometry due to its particulate nature. The LBM-VOF method is the new predictive technique and few reports could be found about its application in pore-scale study on two-phase flow in complex geometry. In this study, two pore-scale models based on above-mentioned two methods are established. The two-phase flow in sub-millimetric pores is numerically predicted and the effect of contact angle is studied based on the numerical prediction.

## 2. Pore Scale Model Based on FVM-VOF Method

### 2.1 Numerical model

The VOF method, which belongs to the Eulerian method, has been widely adopted in

predicting two-phase fluid flows. The VOF formulation relies on the assumption that two fluids are immiscible. For each phase considered in the numerical model, a variable  $F$  is introduced as its volume fraction in the computational cell. In each volume of the computational cells, the volume fractions of two phases sum to unity. Both phases are treated as non-interpenetrating and the flow behavior is described by Navier-Stokes equations.

For a model with two incompressible fluids, the equations for conservation of mass and momentum are:

$$\frac{\partial \rho}{\partial t} + \text{div}(\rho \mathbf{V}) = 0 \quad (1)$$

$$\begin{aligned} \frac{\partial(\rho u)}{\partial t} + \text{div}(\rho u \mathbf{V}) = \\ - \frac{\partial p}{\partial x} + \text{div}(\mu \text{grad } u) + F_{\text{vol},x} \end{aligned} \quad (2)$$

$$\begin{aligned} \frac{\partial(\rho v)}{\partial t} + \text{div}(\rho v \mathbf{V}) = \\ - \frac{\partial p}{\partial y} + \text{div}(\mu \text{grad } v) + F_{\text{vol},y} \end{aligned} \quad (3)$$

$$\begin{aligned} \frac{\partial(\rho w)}{\partial t} + \text{div}(\rho w \mathbf{V}) = \\ - \frac{\partial p}{\partial z} + \text{div}(\mu \text{grad } w) - \rho g + F_{\text{vol},z} \end{aligned} \quad (4)$$

In the numerical model, the liquid and gas (air) are set as the primary and secondary phase, respectively. Tracking of the interface between the phases can be realized by the solution of a continuity equation for the  $F$  of gas, the VOF equation can be given as:

$$\frac{\partial F_g}{\partial t} + \text{div}(F_g \mathbf{V}) = 0 \quad (5)$$

$F_g$  is the volume fraction of gas. If  $F_g = 1$ , the region is pure gas, and if  $F_g = 0$  then the region is pure liquid.  $F_g$  can be between 0 and 1 ( $F_g + F_l = 1$ ), where the interfacial cell exists and all physical properties are mixture ones between the two phases.

The continuum surface force (CSF) model is adopted in this numerical model, in which the

addition of the surface tension results in a volumetric force in the momentum equation. The pressure difference across the interface depends on the surface tension coefficient and the interface curvature as measured by two radii in orthogonal directions,  $r_1$  and  $r_2$ :

$$\Delta p = p_l - p_g = \sigma \kappa \quad (6)$$

in the above equation,  $\Delta p$  is the pressure drop across the interface,  $\sigma$  is the liquid surface tension coefficient and  $\kappa = (1/r_1 + 1/r_2)$  is the mean curvature. In the CSF model, the normal vector on an interface is defined as the gradient of  $F$ :

$$\vec{n} = \nabla F \quad (7)$$

The curvature  $\kappa$  is represented by the divergence of the unit normal as

$$\kappa = \nabla \cdot \frac{\nabla F}{|\nabla F|} \quad (8)$$

The force at the interface can be expressed as a volume force using the divergence theorem, which is the source term added to the momentum equation:

$$F_{\text{vol}} = \sum_{\text{pairs } ij, i < j} \sigma_{ij} \frac{F_i \rho_i \kappa_j \nabla F_j + F_j \rho_j \kappa_i \nabla F_i}{0.5(\rho_i + \rho_j)} \quad (9)$$

for the two phases (gas and liquid) are present in an interfacial cell,  $\kappa_g = -\kappa_l$  and  $\nabla F_g = -\nabla F_l$ , Eq. (9) can be simplified as:

$$F_{\text{vol}} = 2\sigma_{gv} \frac{\rho \kappa_g \nabla F_g}{(\rho_g + \rho_l)} \quad (10)$$

where  $\rho = F_g \rho_g + F_l \rho_l$ .

In this work, one three-dimensional domain with bead porous structure is employed as shown in Fig. 1. The diameter of the beads is assumed to be  $20 \mu\text{m}$ . The inlet and outlet of the porous medium have buffer zone, which spans  $40 \mu\text{m}$  along the flow direction and constant pressure condition is applied at the

inlet/outlet. The length of the edge of the cubical numerical domain is  $50 \mu\text{m}$  each. Boundary walls except the inlet and outlet are treated as no slip condition with the same contact angle. The domain is discretized using the first order upwind scheme for the momentum equations and PRESTO for the continuity equation, the number of grid is about  $9 \times 10^5$  for the whole domain. Transient two-phase simulation starts from an initial condition in which the porous media is partially occupied by stagnant liquid water. The rest part of numerical domain (inlet and outlet buffer area) is full of gas and has constant pressure boundary conditions, which drive the main flow motion in the  $x$ -direction. The time step for transient simulation is fixed at  $10^{-7}$  s and each iteration is assumed to be converged when the absolute criteria of all the governing equations are less than  $10^{-3}$ . The simulation was performed for 3.5 ms and each case takes about one week of computing time using a computer with quad core CPU and sixteen gigabytes of memory.

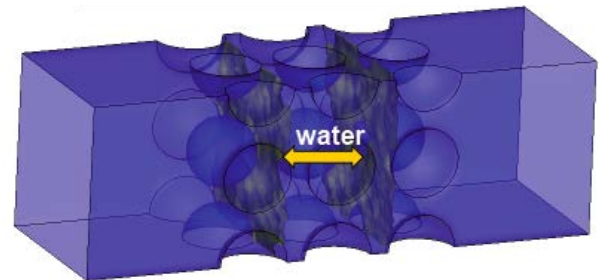
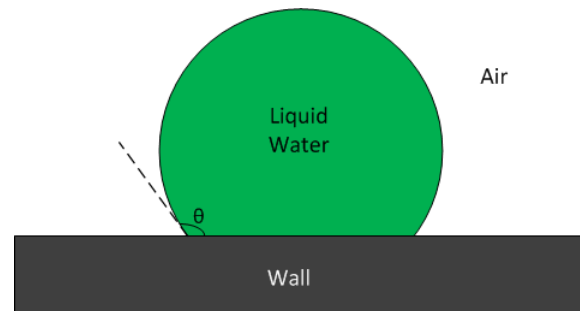
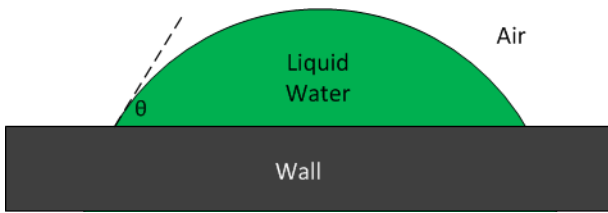


Figure 1. The initial condition (domain size is  $50 \mu\text{m} \times 50 \mu\text{m} \times 140 \mu\text{m}$ )

## 2.2 Numerical results



(a) Hydrophobic



(b) Hydrophilic

Figure 2. Contact angle on the surface

For the porous media with different wettability, different static contact angles are assigned, as shown in Fig. 2. The different contact angles could result in different capillary effect, thus have influence on the liquid water transport.

Figure 3 and 4 present the transient process of liquid water transport in porous media when the pressure inlet is 500 Pa and pressure outlet is 0 Pa. The liquid surface contracts to the minimal area due to the surface tension effect. When the liquid leaves the porous media region, it will move to the bottom due to the gravity effect. In the buffer zone, the surface tension effect is still dominant compared to the gravity effect. It is shown to be a fast liquid transport process for the low surface wettability.

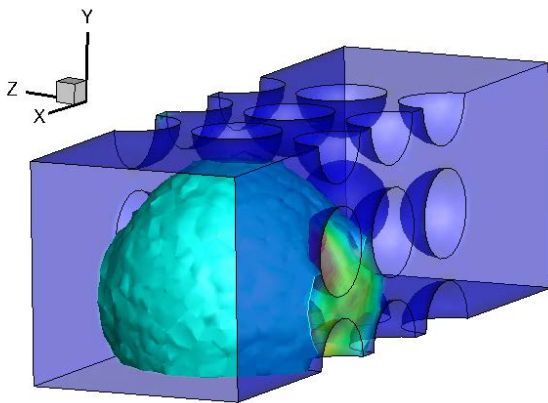
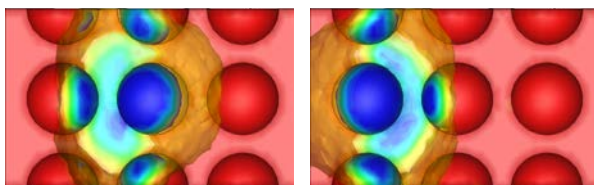
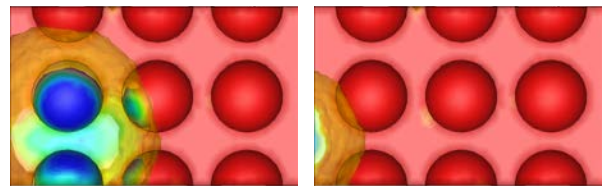


Figure 3. Hydrophobic wall leads to fast transport of water (Contact angle is  $135^\circ$ )



(a)  $t = 0.5 \text{ ms}$

(b)  $t = 1.5 \text{ ms}$



(c)  $t = 2.5 \text{ ms}$

(d)  $t = 3.5 \text{ ms}$

Figure 4. Transient liquid water drainage from the porous media (Contact angle is  $135^\circ$ )

Figure 5 and 6 show the case with hydrophilic boundary walls, in which the same initial condition and pressure boundary conditions are applied. It is shown that the hydrophilic wall leads to a slow removal of water, in which the contact angle is  $45^\circ$ . The water attaches to the boundary wall and it will be a very slow and difficult process for the liquid drainage from the porous media region with high surface wettability.

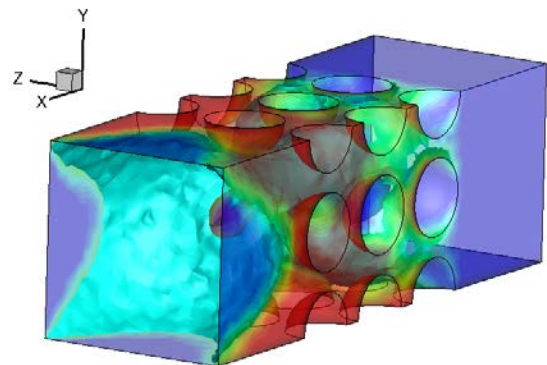
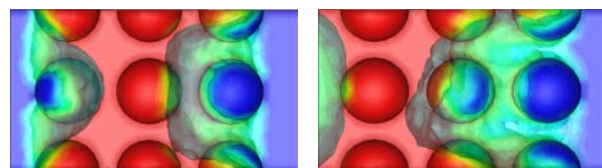
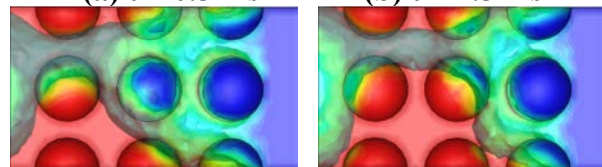


Figure 5. Hydrophilic wall leads to slow transport of water (Contact angle  $45^\circ$ )



(a)  $t = 0.5 \text{ ms}$

(b)  $t = 1.5 \text{ ms}$



(c)  $t = 2.5 \text{ ms}$

(d)  $t = 3.5 \text{ ms}$

Figure 6. Transient liquid water drainage from the porous media (Contact angle is  $45^\circ$ )

### 3. Pore Scale Model Based on LBM-VOF Method

#### 3.1 Numerical method

The Boltzmann equation describes the evolution of particle distribution functions  $f(t, \mathbf{x}, \xi)$ , which specifies the probability to encounter a particle at position  $\mathbf{x}$  at time  $t$  with velocity  $\xi$ :

$$\frac{Df}{Dt} = \frac{\partial f(t, \mathbf{x}, \xi)}{\partial t} + \xi \cdot \frac{\partial f(t, \mathbf{x}, \xi)}{\partial \mathbf{x}} = \Omega \quad (11)$$

The left-hand side of above equation is an advection-type expression, and  $\Omega$  is the collision operator, which describes the interactions of particles on a microscopic scale. For continuum flows with low Knudsen numbers, the directional particle velocities  $e_\alpha$  can be utilized to obtain a set of discrete Boltzmann equations to reduce the computational cost. In the present model, the D3Q19 model is adopted to discretize of the velocity space:

$$\frac{Df_\alpha}{Dt} = \frac{\partial f_\alpha(t, \mathbf{x})}{\partial t} + \mathbf{e}_\alpha \cdot \frac{\partial f_\alpha(t, \mathbf{x})}{\partial \mathbf{x}} = \Omega_\alpha \quad (12)$$

$\alpha = 0, \dots, 18$ . In the model, 18 velocities point to neighboring nodes and one zero velocity. A finite difference discretization in space and time is introduced, on a grid such that  $c = \Delta x / \Delta t = 1$  (grid spacing  $\Delta x$ , time stepping  $\Delta t$ ), which finally leads to the lattice Boltzmann equation:

$$f_\alpha(t + \Delta t, \mathbf{x} + \mathbf{e}_\alpha \Delta t) - f_\alpha(t, \mathbf{x}) = \Omega_\alpha \quad (13)$$

Macroscopic hydrodynamic quantities such as density  $\rho$  and momentum  $\rho_0 \mathbf{V}$  can be obtained from the low order hydrodynamic moments of the distribution functions:

$$\rho = \sum_{\alpha=0}^{18} f_\alpha \quad (14)$$

and

$$\rho_0 \mathbf{V} = \sum_{\alpha=0}^{18} \mathbf{e}_\alpha f_\alpha \quad (15)$$

$\rho_0$  is the reference density.

In this paper, the VOF method is applied for the simulation of free surface flow phenomena. For the solution of the flow field, the LBM is adopted, where the free surface is represented by the VOF approach. The VOF equation (Eq. (5)), is discretized with a finite volume method on the basis of a 3D Piecewise Linear Interface Reconstruction (PLIC) algorithm. The hybrid model is similar with that in (Janen et al., 2013), and only simple geometries were employed in their study and its application was still limited.

The physical model in this work is an inclosure filled with complex foam structure, which is  $151 \mu\text{m} \times 151 \mu\text{m} \times 151 \mu\text{m}$ . The initial liquid water thickness is  $30 \mu\text{m}$ , as shown in Fig. 7. The dark blue surface is the interface between the liquid and gas. The contact angle (foam structure and boundary wall) is  $135^\circ$  and  $45^\circ$ , which are the hydrophobic and hydrophilic boundary condition, respectively.

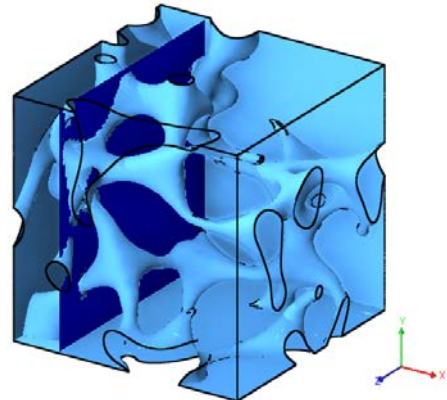


Figure 7. The initial condition (domain size is  $151 \mu\text{m} \times 151 \mu\text{m} \times 151 \mu\text{m}$ )

#### 3.2 Numerical results

It can be found that the water movement varies in the inclosure with different surface wettability. For the hydrophobic surface condition, the liquid contracts to obtain the minimized surface area under the effect of surface tension, as shown in Fig 8. The liquid keeps flowing in the complex pore space and does not attach to the boundary wall of inclosure. The liquid will be easily removed out of the porous media region with the hydrophobic foam structure and boundary wall.

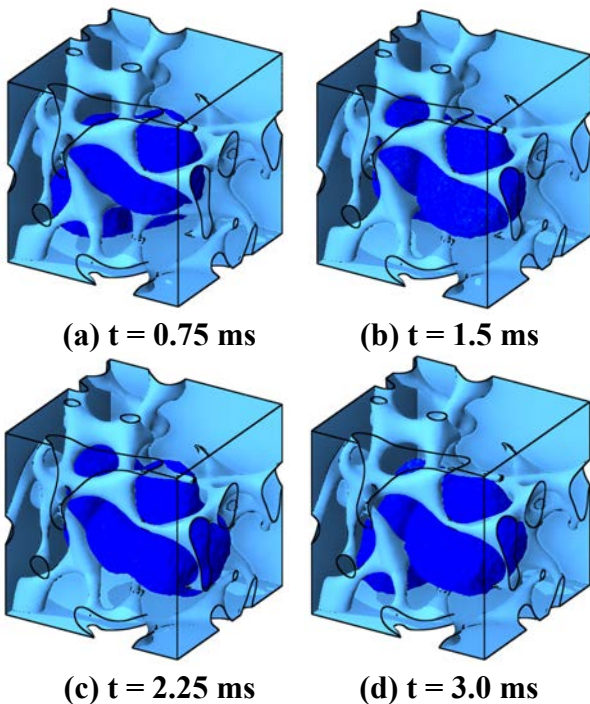


Figure 8. Transient liquid water movement in the porous media (Contact angle is  $135^\circ$ )

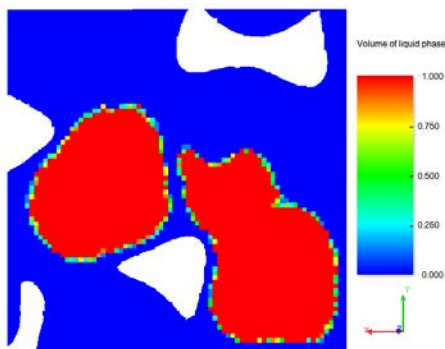


Figure 9. VOF distribution at  $z = 0$  ( $t = 3$  ms)

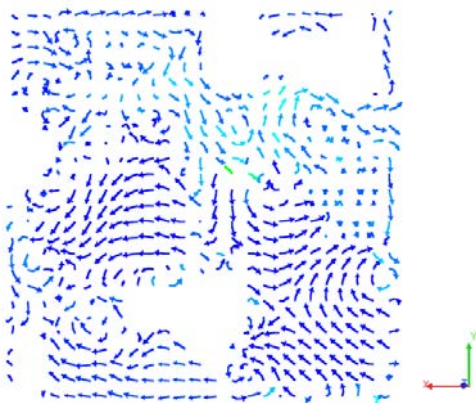


Figure 10. Flow vector at  $z = 0$  ( $t = 3$  ms)

The VOF distribution in the surface of  $z = 0$  ( $t = 3$  ms) is show in Fig.9. The red is liquid, the blue is gas and the empty is where the foam structure exists. The color between red

and blue is where exists the interface of two phases, and its VOF is between 0 (gas) to 1 (liquid). The interface region is limited and is the mixture of the two phases. The corresponding flow vector distribution in the surface of  $z = 0$  ( $t = 3$  ms) is show in Fig.10.

For the hydrophilic surface condition, the liquid moves along the surface of both foam structure and inclosure, which tries to attach on the surface under the effect of adhesive force, as shown in Fig.11. The movement of the liquid water is also influenced by the complex structure of the foam. Then the liquid will be pulled to the corner of the inclosure. Normally, on a mini or micro scale, the liquid will be pulled to the corner of the flow region under the capillary effect, which was pointed out in (Liu et al., 2012).

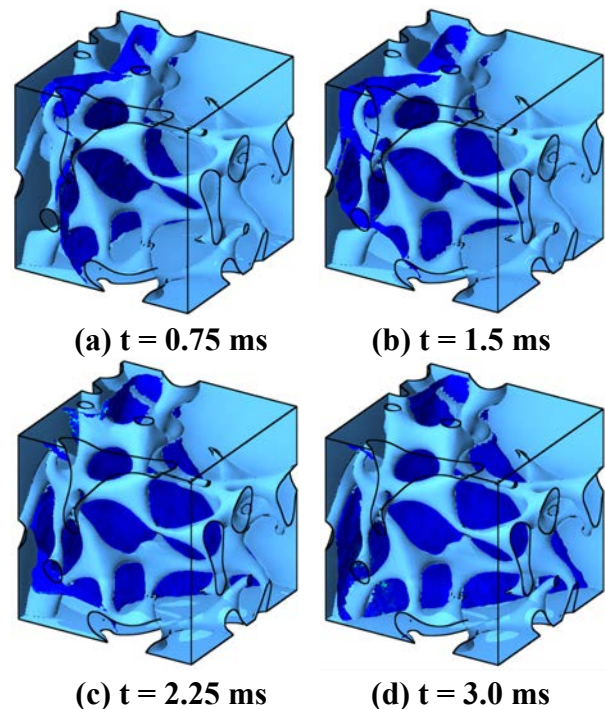


Figure 11. Transient liquid water movement in the porous media (Contact angle is  $45^\circ$ )

In the above two cases, the gravity is along the negative Y-axis direction, which makes the liquid flow to the low part of the domain. But in the domain on micro scale, the gravity is not the dominant force. The capillary force or the surface tension plays the most important role in the two-phase flow.

## 4. Conclusions

Two pore-scale models are established in this paper, which are based on FVM-VOF method and LBM-VOF method, respectively. These two models are both available to simulate the two-phase flow in the pore-scale porous media. The model based on FVM-VOF method will probably meet with meshing problem as the porous structure becomes more complex. The LBM-VOF model has a good advantage in predicting two phase flow in the complex porous media based on its particulate nature. More details and discussion will be provided in the future work.

## Nomenclature

$e$	particle velocity, m/s
$f$	particle distribution functions, -
$F$	volume fraction of fluid (VOF), -
$F_{\text{vol}}$	volume force, N
$g$	gravitational acceleration, m/s <sup>2</sup>
$p$	pressure, N/m <sup>2</sup>
$r$	radius, m
$t$	time, s
$u$	x-velocity, m/s
$v$	y-velocity, m/s
$V$	velocity vector, m/s
$w$	z-velocity, m/s
$x, y, z$	Cartesian coordinates
$x$	position, $(x, y, z)$

## Greek

$\kappa$	interface curvature, 1/m
$\mu$	dynamic viscosity, kg/(m s)
$\xi$	velocity, m/s
$\rho$	density, kg/m <sup>3</sup>
$\sigma$	surface tension, N/m
$\Omega$	collision operator

## Subscripts

0	reference
$g$	gas
$l$	liquid
$x$	x direction
$y$	y direction
$z$	z direction

## Acknowledgements

This paper is supported by the National Natural Science Foundation of China through grant no. 51306119 & 51376130, the National Basic Research Program of China (973 Program) through grant no. 2012CB720404 and Key Basic Research Projects of Science and Technology Commission of Shanghai through grant no. 12JC1405100.

## Reference

- Bandara, U.C., Tartakovsky, A.M., Oostrom, M., Palmer, B.J., Grate, J., Zhang, C., 2013. Smoothed particle hydrodynamics pore-scale simulations of unstable immiscible flow in porous media. *Advances in Water Resources* 62, 356-369.
- Blunt, M.J., Bijeljic, B., Dong, H., Gharbi, O., Iglauer, S., Mostaghimi, P., Paluszny, A., Pentland, C., 2013. Pore-scale imaging and modelling. *Advances in Water Resources* 51, 197-216.
- Gunde, A.C., Mitra, S.K., Babadagli, T., 2010. Pore scale simulation of two-phase fluid flow in Berea Sandstone core using Lattice Boltzmann Method, ASME 2010 8th International Conference on Nanochannels, Microchannels, and Minichannels, ICNMM2010 Collocated with 3rd Joint US-European Fluids Engineering Summer Meeting, August 1, 2010 - August 5, 2010, PARTS A AND B ed. American Society of Mechanical Engineers, Montreal, QC, Canada, pp. 1441-1446.
- Hao, L., Cheng, P., 2010. Pore-scale simulations on relative permeabilities of porous media by lattice Boltzmann method. *International Journal of Heat and Mass Transfer* 53, 1908-1913.
- Janen, C.F., Grilli, S.T., Krafczyk, M., 2013. On enhanced non-linear free surface flow simulations with a hybrid LBM-VOF model. *Computers and Mathematics with Applications* 65, 211-229.
- Jettstuen, E., Helland, J.O., Prodanovic, M., 2013. A level set method for simulating capillary-controlled displacements at the

- pore scale with nonzero contact angles. *Water Resources Research* 49, 4645-4661.
- Jiao, K., Li, X., 2011. Water transport in polymer electrolyte membrane fuel cells. *Progress in Energy and Combustion Science* 37, 221-291.
- Liu, H., Valocchi, A.J., Kang, Q., Werth, C., 2013. Pore-Scale Simulations of Gas Displacing Liquid in a Homogeneous Pore Network Using the Lattice Boltzmann Method. *Transport in Porous Media* 99, 555-580.
- Liu, Z., Sunden, B., Yuan, J., 2012. Numerical simulation of condensation in a rectangular minichannel using VOF model, ASME 2012 International Mechanical Engineering Congress and Exposition, IMECE 2012, November 9, 2012 - November 15, 2012, PARTS A, B, C, D ed. American Society of Mechanical Engineers, Houston, TX, United states, pp. 2577-2583.
- Raeini, A., Bijeljic, B., Blunt, M., 2014. Numerical Modelling of Sub-pore Scale Events in Two-Phase Flow Through Porous Media. *Transport in Porous Media* 101, 191-213.
- Shahraeeni, E., Or, D., 2012. Pore-scale evaporation-condensation dynamics resolved by synchrotron x-ray tomography. *Physical Review E - Statistical, Nonlinear, and Soft Matter Physics* 85.
- Sheng, Q., Thompson, K., 2013. Dynamic coupling of pore-scale and reservoir-scale models for multiphase flow. *Water Resources Research* 49, 5973-5988.
- Shokri, N., Lehmann, P., Or, D., 2010. Liquid-phase continuity and solute concentration dynamics during evaporation from porous media: Pore-scale processes near vaporization surface. *Physical Review E - Statistical, Nonlinear, and Soft Matter Physics* 81.
- Xuan, Y., Zhao, K., Li, Q., 2011. Investigation on Heat and Mass Transfer in a Evaporator of a Capillary-Pumped Loop with the Lattice Boltzmann Method: Pore Scale Simulation. *Transport in Porous Media* 89, 337-355.